

## Supporting Information

### Ruthenium-based Metal-Organic Framework Catalyst for CO<sub>2</sub> Fixation onto Epoxides

James Ho<sup>1</sup>, Makenzie T. Nord<sup>1</sup>, Jared P. Stafford<sup>1</sup>, Kyriakos C. Stylianou<sup>1\*</sup>

<sup>1</sup>Materials Discovery Laboratory (MaD Lab), Department of Chemistry, Oregon State University,  
Corvallis, Oregon, United States, 97331

Email: [kyriakos.stylianou@oregonstate.edu](mailto:kyriakos.stylianou@oregonstate.edu)

## Table of Contents

SI 1. Experimental.....	3
SI 1.1. Materials.....	3
SI 1.2. Synthetic Protocols.....	3
SI 1.2.1 Synthesis of Ru <sub>2</sub> (OAc) <sub>4</sub> Cl.....	3
SI 1.2.2 Synthesis of Ru <sup>II/III</sup> HKUST-1 and Cu-HKUST-1.....	3
SI 1.3. Characterization Protocols.....	4
SI 1.3.1. Powder X-Ray Diffraction.....	4
SI 1.3.2. Fourier Transform Infrared Spectroscopy .....	4
SI 1.3.3 UV/Vis Diffuse Reflectance.....	4
SI 1.3.4. Thermogravimetric Analysis.....	4
SI 1.3.5. Nitrogen Adsorption Isotherm.....	4
SI 1.3.6. Solvent Stability.....	4
SI 2. Characterization.....	5
SI 2.1. Powder X-Ray Diffraction.....	5
SI 2.2. Fourier Transform Infrared Spectroscopy.....	5
SI 2.3. UV/Vis Diffuse Reflectance.....	6
SI 2.4. Thermogravimetric Analysis.....	6
SI 2.5. Nitrogen Adsorption Isotherm.....	7
SI 2.6. Solvent Stability.....	7
SI 3. Catalysis Experiments.....	8
SI 3.1. Catalytic Procedure.....	8
SI 3.2. <sup>1</sup> H NMR Spectra Qualification.....	9
SI 3.3. <sup>1</sup> H NMR Spectra Quantification.....	13
SI 3.4. Catalytic Performance for Propylene Oxide.....	14
SI 3.4.1. Catalytic optimization for Propylene Oxide.....	14
SI 3.5. Catalysis Experiments for Various Epoxides .....	15
SI 3.6. Recyclability and Post Catalysis.....	16
SI 3.6.1. Fourier Transform Infrared Spectroscopy Post Catalysis.....	16
SI 3.6.2. Catalytic Recyclability.....	16
SI 4. Literature Comparison .....	17
SI 5. References .....	18

## SI 1. Experimental

### SI 1.1. Materials

Propylene oxide (PO) ( $\geq 99\%$ ), 1,2-dimethoxyethane (DME) (99.5%), tetramethylammonium bromide (TBAB) (98%), (EtOH) (99.5%), ruthenium trichloride hydrate ( $\text{RuCl}_3$ , 40 – 49 % Ru content), and acetic acid ( $\geq 99\%$ ), were purchased from Sigma Aldrich. Copper (II) dichloride ( $\text{CuCl}_2$ ) was purchased from Honeywell. Glycidol (GLY) ( $\geq 99\%$ ) was purchased from Fisher Scientific. Epichlorohydrin (ECH) ( $\geq 99\%$ ), Styrene oxide (SO) ( $\geq 99\%$ ), 1,2-butylene oxide (BO) ( $\geq 99\%$ ), cyclohexene oxide (CHO) ( $\geq 99\%$ ) and 1,3,5-benzene tricarboxylic acid (1,3,5-BTC) were purchased from TCI.  $\text{CO}_2$  was purchased from Airgas (99.999 %  $\text{CO}_2$ ). All the above chemicals were used without further purification.

### SI 1.2. Synthetic Protocols

#### SI 1.2.1. Synthesis of Ru-acetate ( $\text{Ru}_2(\text{OAc})_4\text{Cl}$ )

Ru-acetate was synthesized following a previously reported literature procedure with few modifications. Briefly, glacial acetic acid (36 mL), acetic anhydride (8 mL), and anhydrous LiCl (1 g, 25.2 mmol) were added to a two-neck round bottom flask equipped with a water condenser.  $\text{O}_2$  was bubbled into the solution for approximately 1 hour, after which  $\text{RuCl}_3$  hydrate (1 g, 4.8 mmol) was added. The temperature was increased to  $50^\circ\text{C}$  for 30 minutes, then heated to reflux ( $160^\circ\text{C}$ ) overnight with continued  $\text{O}_2$  bubbling. After cooling to room temperature, the  $\text{O}_2$  bubbling was stopped, and the product ( $\text{Ru}_2(\text{OAc})_4\text{Cl}$ ) was collected by centrifugation and washed with acetic acid (3x) and diethyl ether (1x) and left to air dry.

#### SI 1.2.2. Synthesis of $\text{Ru}^{\text{II/III}}$ HKUST-1 and Cu-HKUST-1

Ru-HKUST-1 MOF was synthesized following a slightly modified procedure from Lorz et al.. The previously synthesized Ru-acetate ( $\text{Ru}_2(\text{OAc})_4\text{Cl}$ , 0.310 g, 0.654 mmol), 1,3,5-benzene tricarboxylic acid (0.182 g, 0.866 mmol), glacial acetic acid (1.2 mL) and DI water (7.3 mL) were combined in a 25 mL Teflon liner and stirred for  $\sim 10$  min using a magnetic stir plate. The liner was inserted into the Parr bomb body, sealed, and placed in a preheated  $160^\circ\text{C}$  oven for 72 h, with a cool down ramp rate of  $0.20^\circ\text{C}/\text{min}$ . The product was collected by centrifugation and washed with DI water (4x) and methanol (1x). A methanol solvent exchange was performed for three days. Cu-HKUST-1 was synthesized exactly the same, except  $\text{CuCl}_2 \cdot 2\text{H}_2\text{O}$  (0.11 g, 0.654 mmol) was used as the metal salt.

### **SI 1.3. Characterization Protocols**

#### **SI 1.3.1. Powder X-Ray Diffraction**

PXRD data were collected using a Rigaku Miniflex 600 diffractometer (monochromated Cu K $\alpha$  radiation,  $\lambda = 1.54178 \text{ \AA}$ ) with a tube voltage and current of 40 kV and 15 mA, respectively. Data was collected over the  $2\theta$  range of  $3^\circ - 30^\circ$  at a scan rate of 0.075 degrees/min with a  $0.02^\circ$  step at ambient conditions.

#### **SI 1.3.2. Fourier Transform Infrared Spectroscopy**

All FT-IR measurements were performed on a PerkinElmer Spectrum Two Spectrometer equipped with a Universal Attenuated Total Reflectance (UATR) accessory tool (single reflection diamond). Spectra were obtained with a resolution of  $4 \text{ cm}^{-1}$  from  $400 - 4000 \text{ cm}^{-1}$  and averaged over eight scans.

#### **SI 1.3.3. UV-Vis Absorbance and Diffuse Reflectance**

Diffuse reflectance spectra were obtained using a PerkinElmer UV/Vis/NIR Lambda 1050+ spectrometer equipped with a 100 mm integrating sphere and acquired in the 200 – 800 nm range. Powder samples were deposited in a solid sample holder equipped with a quartz window, and a Spectralon reflectance standard was used as the reference. The Kubelka-Munk (K-M) function was applied to the raw spectral data.

#### **SI 1.3.4. Thermogravimetric Analysis**

TGA was performed using a standard TG-DTA analyzer from Hiden Analytical. Approximately 7-10 mg of the sample was placed in a TGA crucible. The samples were heated from  $25^\circ\text{C} - 650^\circ\text{C}$  at  $10^\circ\text{C}/\text{min}$  under argon (100 ml/min).

#### **SI 1.3.5. Nitrogen Adsorption Isotherms**

$\text{N}_2$  sorption isotherms were collected using a 3FLEX Adsorption Analyzer from Micromeritics. Prior to analysis, the samples were activated overnight at  $100^\circ\text{C}$ . The Brunauer-Emmett-Teller (BET) surface areas were estimated from the amount of  $\text{N}_2$  adsorbed at 77 K and 1 bar using the BET equilibrium equation.

#### **SI 1.3.6. Solvent Stability**

To test the stability of the MOF in varying solvents, approximately 10.0 mg of Ru-HKUST-1 was submerged in 1.0 mL of solvent for 24 hours. The samples were then filtered and air-dried overnight before stability was checked with PXRD. This procedure was repeated for every solvent tested.

## SI 2. Characterization

### SI 2.1 Powder X-Ray Diffraction

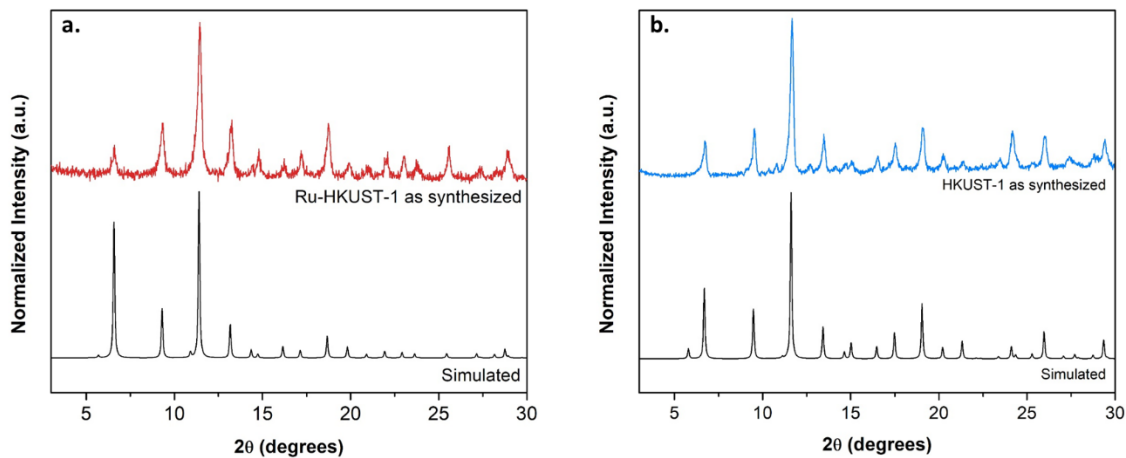


Figure S1a-b. PXRD patterns of (a) Ru-HKUST-1 and (b) HKUST-1.

### SI 2.2 Fourier Transform Infrared Spectroscopy

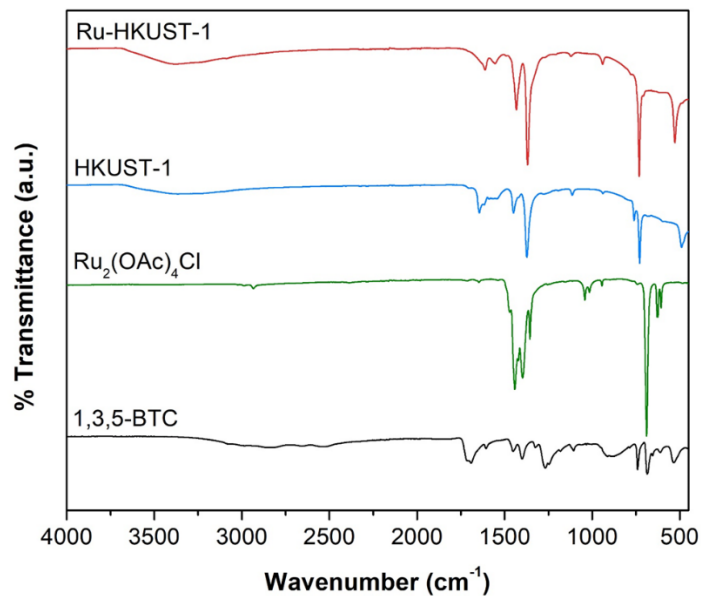
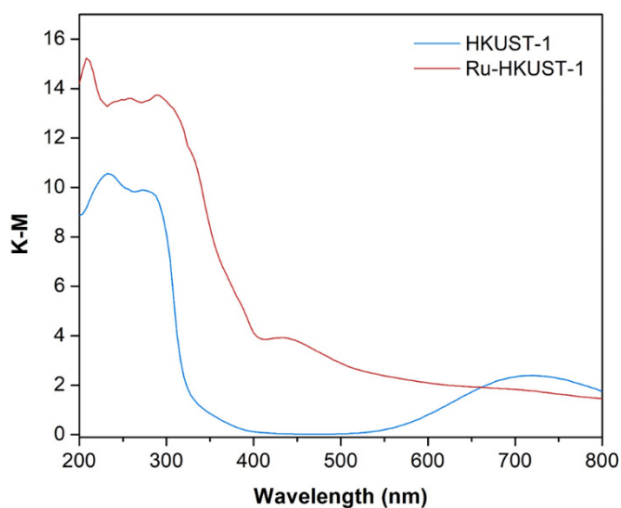


Figure S2. FT-IR plots of Ru-HKUST-1, HKUST-1, Ru-acetate, and 1,3,5-BTC.

### SI 2.3. UV/Vis and Diffuse Reflectance Spectra



**Figure S3.** Kubelka-Munk representation of the Diffuse Reflectance data for each MOF.

### SI 2.4. Thermogravimetric Analysis

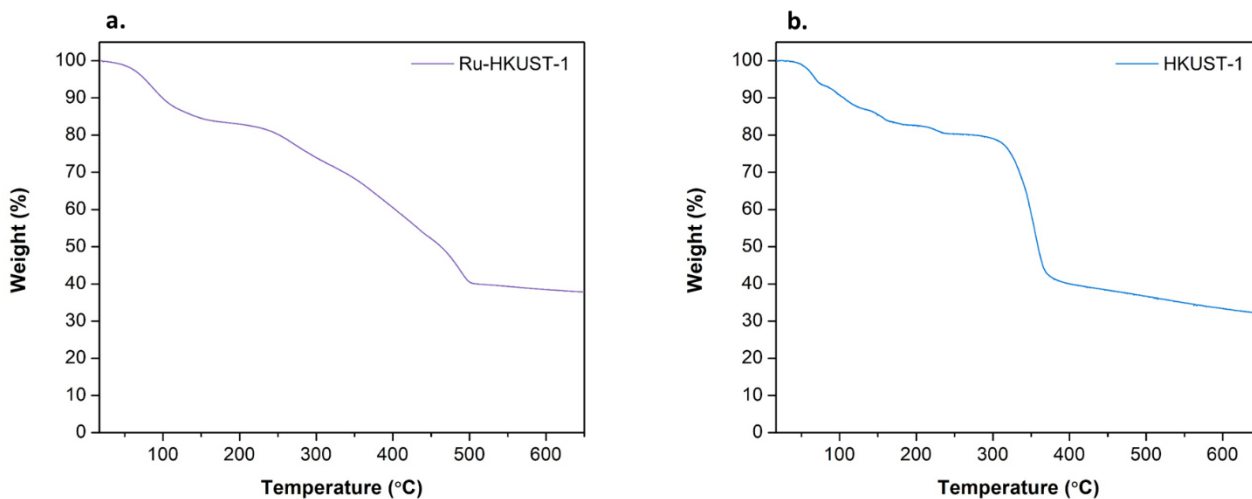


**Figure S4a-b.** TGA plot of Ru-HKUST-1 (a) and HKUST-1 (b). Ru-HKUST-1 is stable up to ~225°C and HKUST-1 is stable up to ~300°C.

## SI 2.5. Nitrogen Adsorption Isotherm

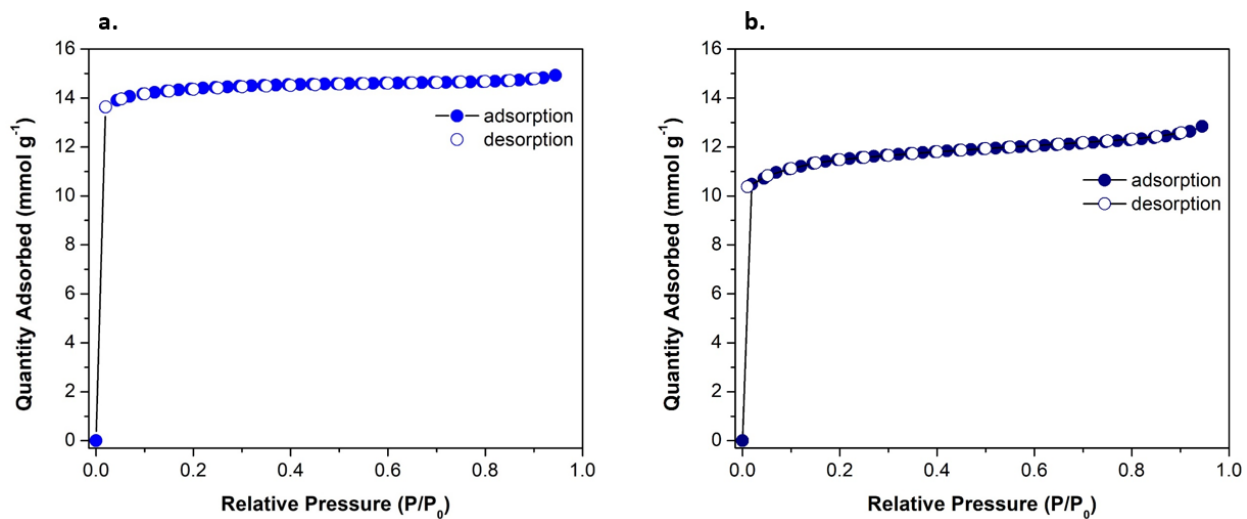


Figure S5. N<sub>2</sub> adsorption isotherm at 77K for Ru-HKUST-1 (a.) and HKUST-1(b.)

## SI 2.6. Solvent Stability

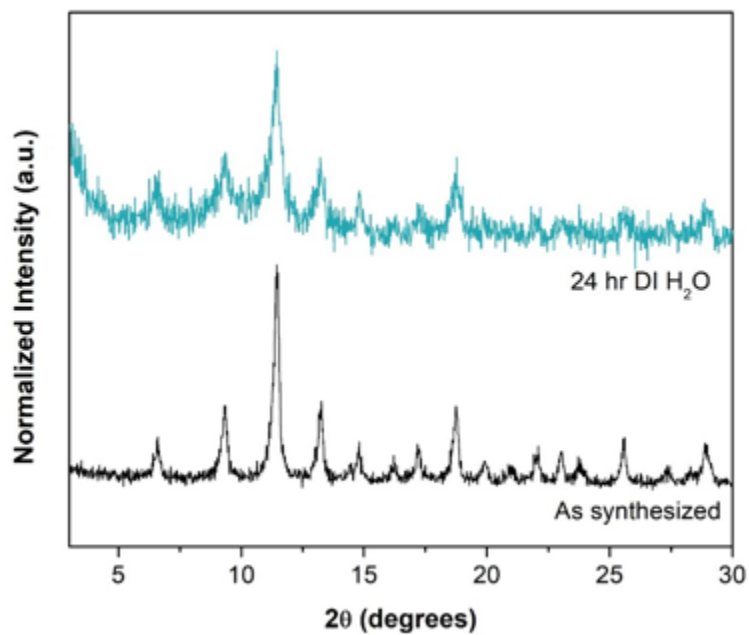


Figure S6 PXRD of Ru-HKUST-1 before and after submerged in DI water for 24 hours.

### SI 3. Catalysis Experiments

#### SI 3.1. Catalytic Procedures

##### *Optimized procedure*

[Ru-HKUST-1] (20.6 mg, 0.03125 mmol), tetramethylammonium bromide (TBAB, 290.0 mg, 0.900 mmol), 1,2- dimethoxyethane (DME, 2.50 mL, 24.05 mmol), and propylene oxide (PO, 2.50 mL, 35.7 mmol) were added to a 50 mL stainless steel autoclave reactor (Parr Instruments Series 4790). The reactor was pressurized to 7 bar with 99.99 % CO<sub>2</sub> before heating it to 50 °C for 24 hours. After 24 hours, a 25 μL aliquot was taken from the reaction solution and syringe filtered for <sup>1</sup>H NMR analysis to determine the conversion of propylene oxide to propylene carbonate. The remaining solution was vacuum filtered to recover the catalyst and sequentially washed acetone (2x) and DI H<sub>2</sub>O (2x). The recovered catalyst was then vacuum dried overnight to be used for the next cycle.

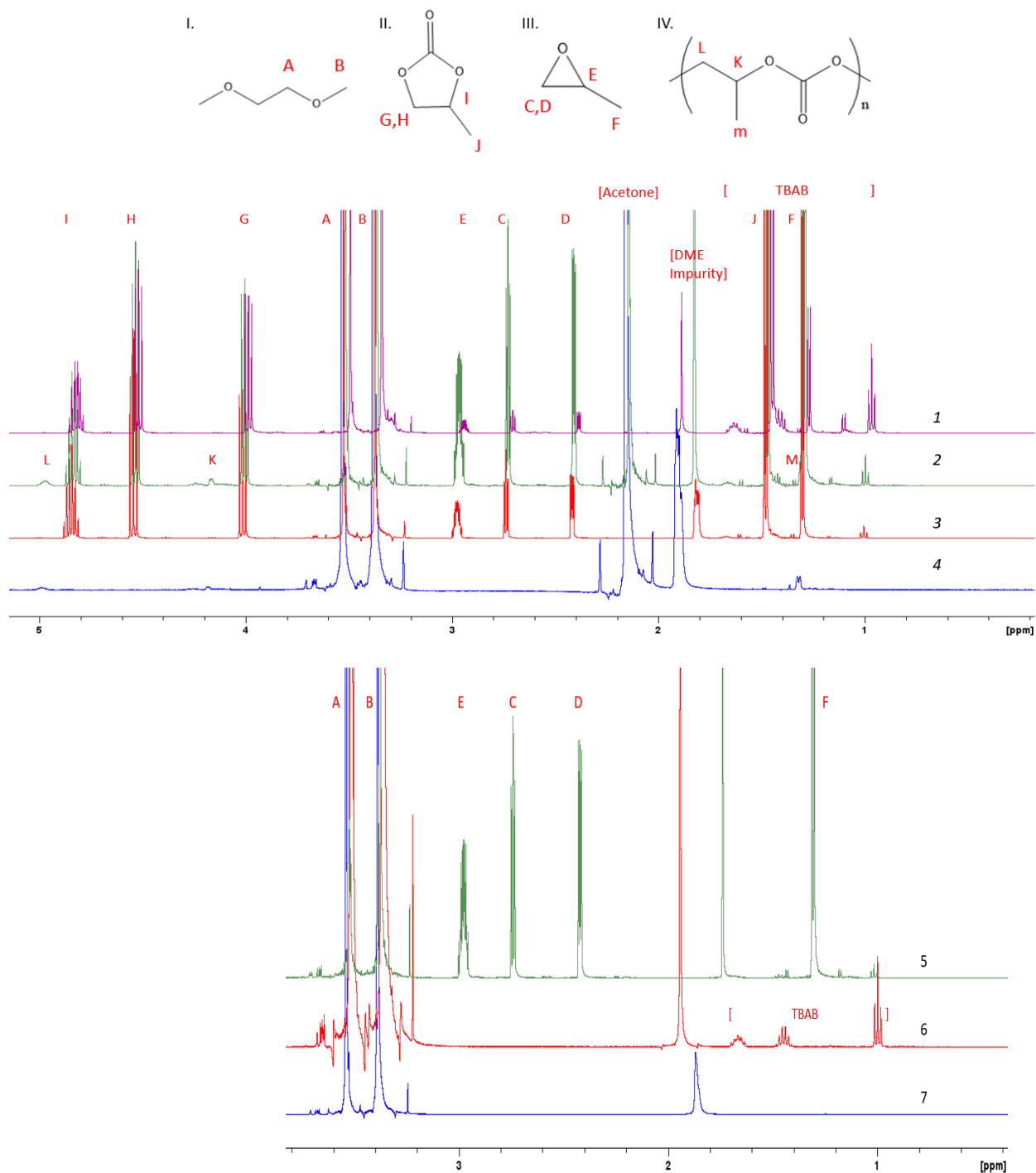
##### *Varying the Mole Ratio*

The procedure above was followed, with the exception that for every epoxide, the experiments were performed with either 12 mmol of epoxide (1:1 [epoxide: CO<sub>2</sub>] ratio) or 4 mmol of epoxide (1:3 [epoxide: CO<sub>2</sub>] ratio).



### SI 3.2. <sup>1</sup>H NMR Spectra Qualification

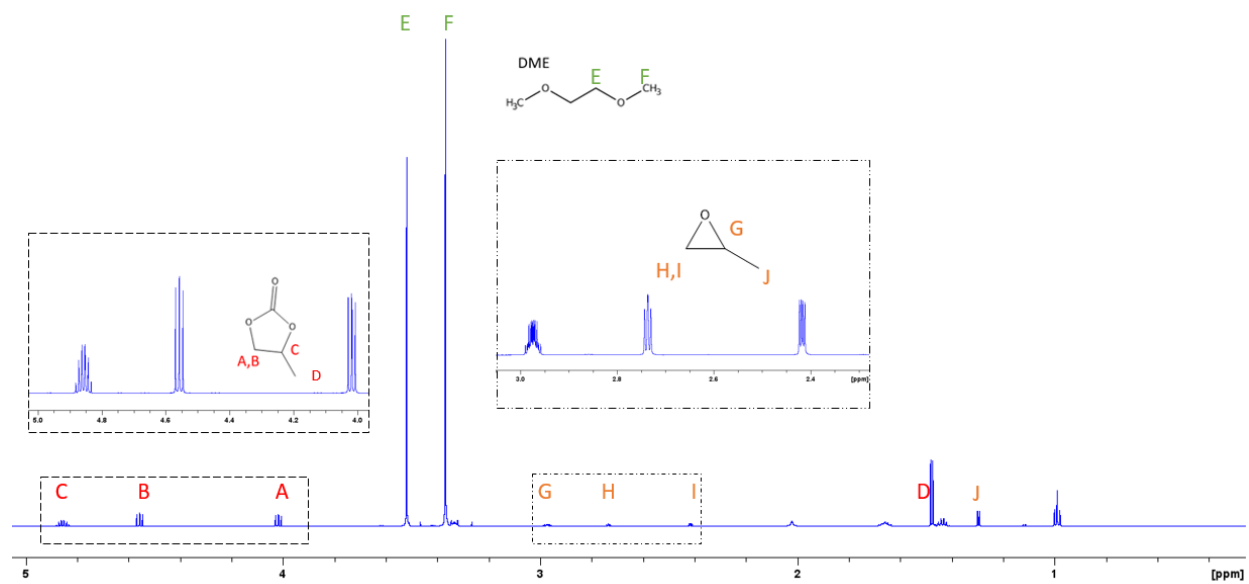
#### Control <sup>1</sup>H NMR



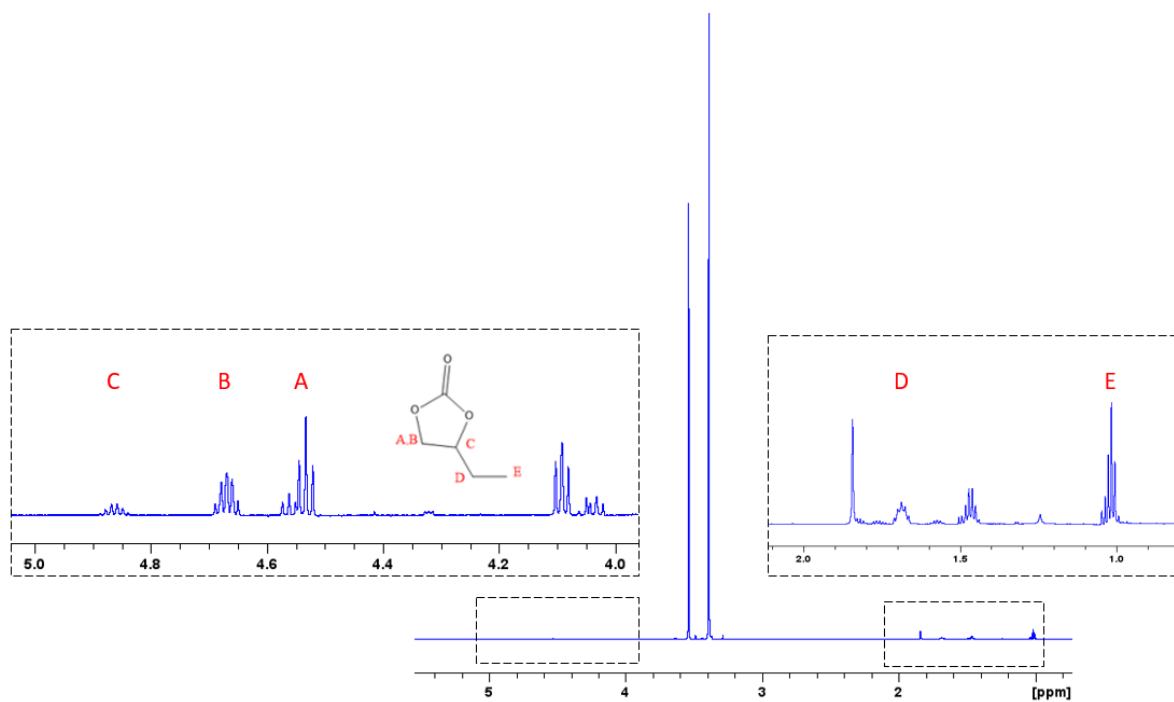
I. 1,2-dimethoxyethane (DME) II. Propylene Carbonate (PC) III. Propylene Oxide (PO) IV. Poly(Propylene Carbonate) (PPC) 1. *in situ* 2. DME/Acetone/TBAB/PO/PC/PPC 3. DME/TBAB/PO/PC 4. DME/Acetone/PPC 5. DME/TBAB/PO 6. DME/TBAB 7. DME

## *In situ* $^1\text{H}$ NMR

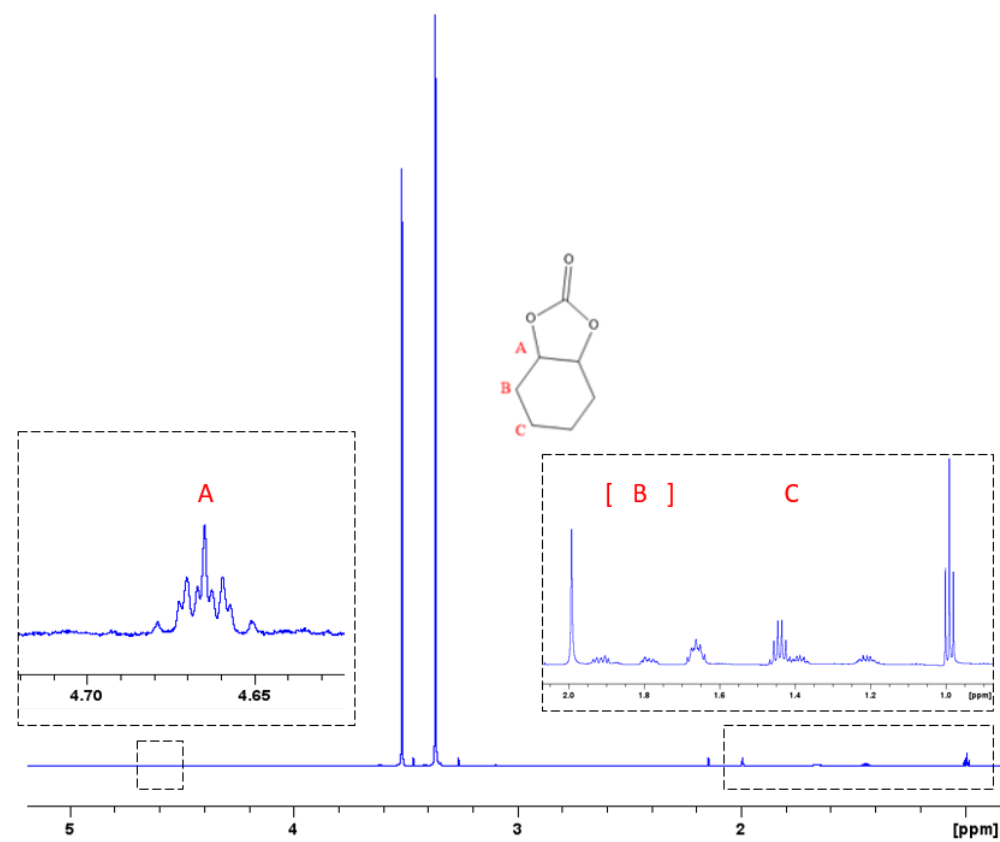
### a. Propylene Carbonate



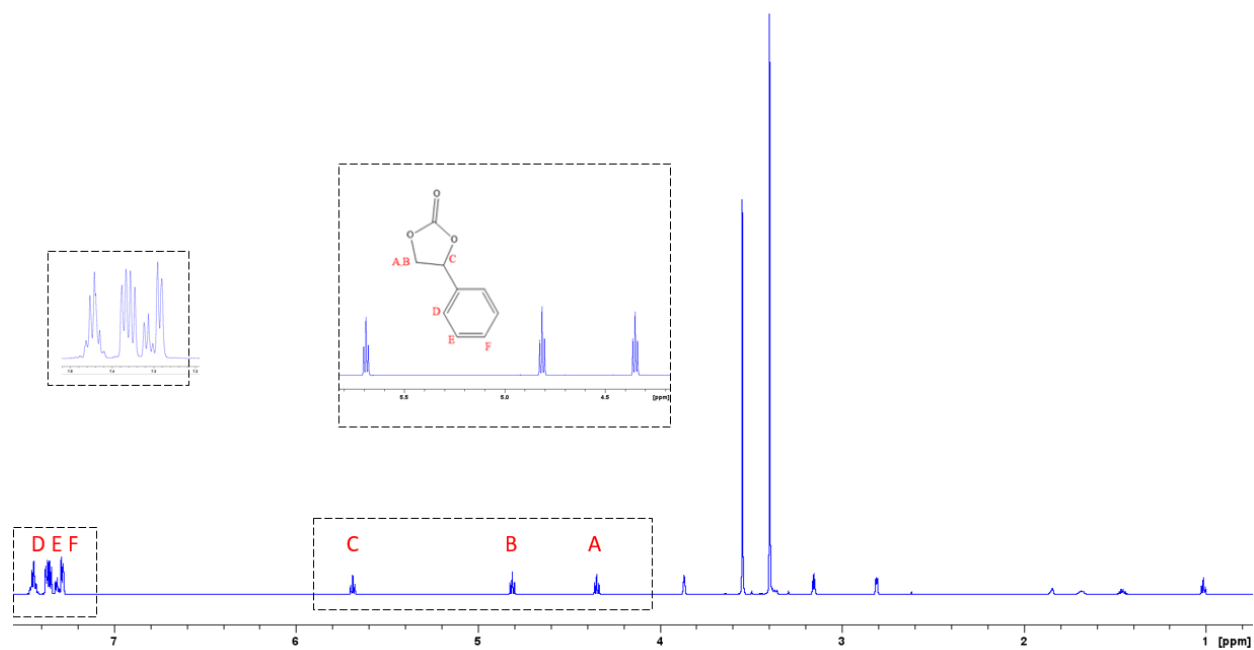
### b. Butylene Carbonate



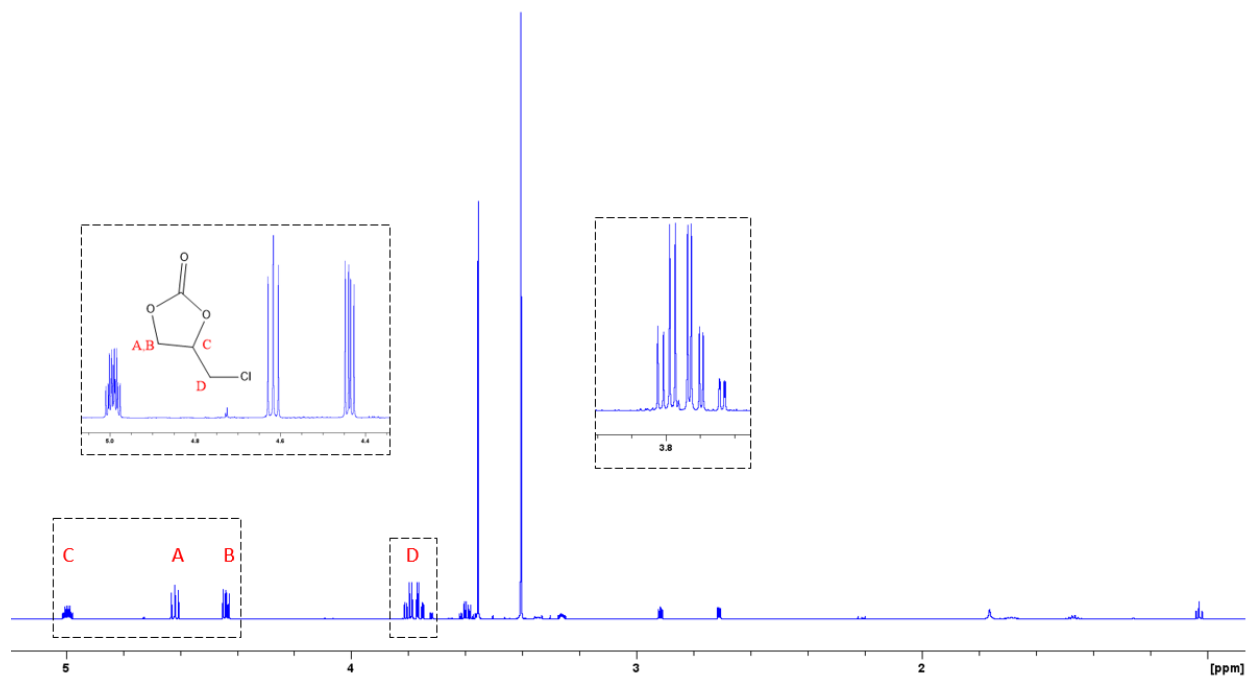
### c. Cyclohexene Carbonate



### d. Styrene Carbonate



### e. Epichlorohydrin Carbonate



### f. Glycerol Carbonate

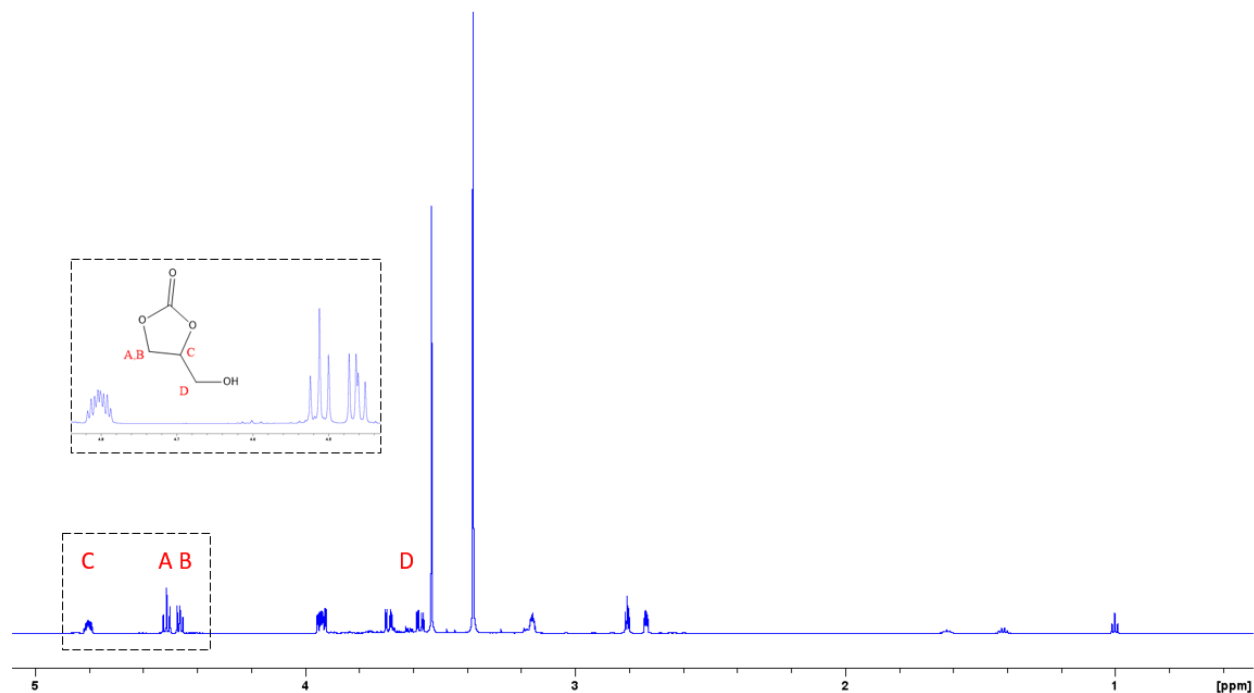


**Figure S7a-f.**  $^1\text{H}$  NMR ( $\text{CDCl}_3$ , 500 MHz) spectra showing peaks of propylene oxide (orange), propylene carbonate (red), and DME (green). All other residual peaks are due to TBAB (unlabeled), acetone

(unlabeled) , impurities within DME solvent or satellite peaks of existing substances (unlabeled) (a). All proceeding  $^1\text{H}$  NMR spectra only label the protons of their respective carbonate structures (b-f).

### SI 3.3. $^1\text{H}$ NMR Spectra Quantification

The yield of cyclic carbonate was determined by  $^1\text{H}$  NMR. A 25  $\mu\text{L}$  aliquot was extracted from the solution and mixed with 575  $\mu\text{L}$  of deuterated chloroform ( $\text{CDCl}_3$ ) in a 5mm NMR tube. The spectra were analyzed using a 500 MHz Bruker Avance spectrometer equipped with a BBO probe.

Only the ring protons of each cyclic carbonate and the protons of 1,2-dimethoxyethane (DME) were considered for the following calculations. The ratio of cyclic carbonate to DME was calculated from the integration areas determined from the  $^1\text{H}$  NMR spectra.

$$\frac{M_{\text{Carbonate}}}{M_{\text{DME}}} = \left( \frac{I_{\text{Carbonate}}}{I_{\text{DME}}} \right) \left( \frac{N_{\text{DME}}}{N_{\text{Carbonate}}} \right)$$

I = Integral Area

N = Number of Nuclei

M = Number of Moles

The initial molar amount of DME (16.9 mmol) was held constant through the reaction and is used to determine the total molar amount of carbonate formed.

$$M_{\text{Carbonate,Total}} = \left( \frac{M_{\text{Carbonate}}}{M_{\text{DME}}} \right) (M_{\text{DME,Total}})$$

Conversion is calculated by comparing the final amount of carbonate calculated to the initial amount of limiting reagent (LR). (1:3 and 1:1 LR = epoxide, 3:1 LR=  $\text{CO}_2$ ). The M of catalyst (0.03125 mmol) and time (24h) were held constant for every trial when calculating TON and TOF.

$$\text{Conversion} = \left( \frac{M_{\text{carbonate,Total}}}{M_{\text{LR}}} \right) (100\%)$$

$$\text{TON} = \left( \frac{M_{\text{carbonate}}}{M_{\text{catalyst}}} \right)$$

$$\text{TOF} = \left( \frac{\text{TON}}{\# \text{ hours}} \right)$$

### SI 3.4. Catalytic Performance for Propylene Oxide

#### SI 3.4.1. Catalytic Optimization for Propylene Oxide

**Table S1.** PO conversion at varying temperatures\*

Temperature (C)	Pressure [Bar]	Cu-HKUST-1	Ru-HKUST-1
65	10	80%	91%
45	10	47%	86%
25	10	5%	11%

**Table S2.** PO Conversion at varying pressures\*

Temperature (C)	Pressure [Bar]	Catalyst	Conversion
50	13	Ru-HKUST-1	55%
50	10	Ru-HKUST-1	86%
50	7	Ru-HKUST-1	93%
50	4	Ru-HKUST-1	49%
50	1	Ru-HKUST-1	56%
50	7	Cu-HKUST-1	46%

\* Optimization conditions; 50 mL autoclave stainless-steel autoclave reactor, 0.03125 mmol catalyst, solvent (2.50 mL, 24.0 5mmol DME), reaction time = 24h.

### SI 3.5. Catalysis Experiments for Various Epoxides

**Table S3.** The conversion of epoxide to cyclic carbonate depends on the amount of limiting reagent (epoxide) present before reaching equilibrium. Equimolar ratios of epoxide to CO<sub>2</sub> show little difference in conversion despite their different concentration loadings and increased reaction times.

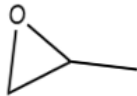
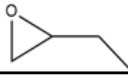
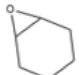
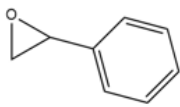
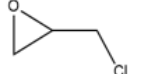
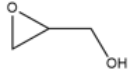
CO <sub>2</sub> Loading	Epoxide Loading	Time	% Conversion Styrene Oxide	% Conversion Propylene Oxide
7 bar (12 mmol)	12 mmol	24 hours	23%	15%
15 (27.9 mmol)	27.9 mmol	24 hours	29%	25%
25 (44 mmol)	44 mmol	96 hours	-	28%

\*CO<sub>2</sub> loading was calculated using Van Der Waals equation. The volume occupied by the gas was measured by taking the difference between the total volume of the autoclave and the volume occupied by the solvents.

**Table S4.** Table showing yield, TON, TOF, and pressure loss for epoxides with varying molar reactant ratios under optimized temperature and pressures<sup>a</sup>.

50 C, 7 Bar

**Table 1.** Percent conversion, TON and TOF for various epoxides in different reactant ratio<sup>a</sup>

Epoxide	Catalyst	Ratio [epoxide: CO <sub>2</sub> ]	P <sub>initial</sub> [bar]	P <sub>final</sub> [bar]	Conversion [%]	TON [mmol/ mmol cat]	TOF [mmol/ mmol cat*hr]
	Ru-HKUST-1	3:1	7	4	93.2%	1319.0	54.9
	Cu-HKUST-1	3:1	7	4	45.9%	629.8	31.5
	No Cat	3:1	7	5	19.4%	223.1	9.3
	Ru-HKUST-1	1:1	7	6	15.3%	226.8	9.5
	No Cat	1:1	7	7	11.3%	70.1	2.9
	Ru-HKUST-1	1:3	7	7	14.3%	19.8	0.8
	Ru-HKUST-1	3:1	7	4	72.5%	665.2	26.6
	Ru-HKUST-1	1:1	7	7	4.5%	18.9	0.8
	Ru-HKUST-1	1:3	7	7	7.5%	10.6	0.4
	Ru-HKUST-1	3:1	7	6	51.9%	409.0	16.4
	Ru-HKUST-1	1:1	7	7	7.3%	31.2	1.3
	Ru-HKUST-1	1:3	7	7	6.9%	9.7	0.4
	Ru-HKUST-1	3:1	7	0	79.0%	852.2	35.5
	Cu-HKUST-1	3:1	7	1	48.9%	344.3	14.4
	Ru-HKUST-1	1:1	7	6	22.8%	87.5	3.7
	Ru-HKUST-1	3:1	7	0	97.2%	994.0	41.4
	Ru-HKUST-1	1:1	7	5	25.2%	103.3	4.3
	Ru-HKUST-1	1:3	7	4	37.6%	53.0	2.2
	Ru-HKUST-1	3:1	7	0	56.8%	681.9	28.4
	Ru-HKUST-1	1:1	7	7	13.5%	53.9	2.3
	Ru-HKUST-1	1:3	7	7	10.9%	15.6	0.7

<sup>a</sup> Reaction conditions; 50 mL autoclave stainless-steel autoclave reactor, 0.03125 mmol catalyst (if present), solvent (2.50 mL, 24.05mmol DME), 50°C, 7 bar pure CO<sub>2</sub>, reaction time = 24h.

### SI 3.6. Recyclability and Post Catalysis

#### SI 3.6.1. Fourier Transform Infrared Spectroscopy Post Catalysis

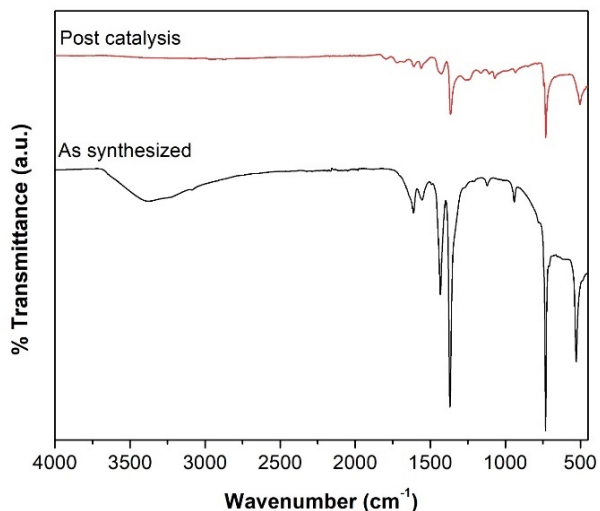


**Figure S8.** Ru-HKUST-1 post catalysis FT-IR (3<sup>rd</sup> cycle), confirming retained functional groups

#### SI 3.6.2. Catalytic Recyclability

**Table S5.** Post catalysis runs for the cycloaddition of CO<sub>2</sub> onto epichlorohydrin (ECH) under the optimized conditions. Yield and recovered amount of Ru-HKUST-1 is reported.

Cycle	Epoxide	Recovered [%]	Conversion [%]	Selectivity [%]
1	ECH	100	97	>99
2	ECH	100	99	>99
3	ECH	97	90	>99
4	ECH	75	83	>99



## SI 4. Literature Comparison

**Table S6.** Comparison of MOFs/COFs reported using TBAB coupled PO to PC conversion.

Material	Temperature [°C]	CO <sub>2</sub> Pressure [Bar]	Time [hr]	TOF [hr <sup>-1</sup> ]	Yield [%]	Reference
MMCF-2	25	1	48	4	49	<a href="#">1</a>
{[Zn(H <sub>2</sub> O)(HL)]·(DMF) <sub>2</sub> (H <sub>2</sub> O) <sub>2</sub> } <sub>n</sub>	25	1	48	-	76	<a href="#">2</a>
MOF-505	25	1	48	4	49	<a href="#">1</a>
In <sub>2</sub> (OH)(btc)(Hbtc) <sub>0.4</sub> (L) <sub>0.6</sub> ·3H <sub>2</sub> O	25	1	48	7.1	78	<a href="#">3</a>
OMe-OH-TPBP-COF.	40	1	24	-	90	<a href="#">4</a>
Cu <sub>x</sub> O <sub>y</sub> @COF	40	1	12	-	92	<a href="#">5</a>
MOF-5	50	60	4	36.4	95	<a href="#">6</a>
UiO-66-BAT	50	5	12	-	40	<a href="#">7</a>
Ru-HKUST-1	50	7	24	54.9	93	This Work
HKUST-1	50	7	24	31.5	55	This Work
NUC-51a	55	1	6	16.5	99	<a href="#">8</a>
TbL	70	10	12	2.4	45	<a href="#">9</a>
NUC-53	80	1	4	-	99	<a href="#">10</a>
ZIF-8	80	8	5	-	68	<a href="#">11</a>
ZIF-67	80	8	5	-	55	<a href="#">11</a>
Cu <sub>2</sub> BPDSDC	80	25	5	19.1	>99	<a href="#">2</a>
Ce[HTCPB]	100	10	12	20	>99	<a href="#">12</a>
NH <sub>2</sub> -Mil-101(Al)	120	18	6	22	96	<a href="#">13</a>
UMCM-1-NH <sub>2</sub>	120	12	24	5.9	41	<a href="#">14</a>
Pt/Mg-MOF-74	150	17.5	4	-	44	<a href="#">15</a>

- = not reported

**Table S7.** Comparison of MOFs/COFs from literature for various cyclic carbonate conversions<sup>a</sup>

Yield [%] for various substrates to cyclic carbonates

Material	Temperature [°C]	CO <sub>2</sub> Pressure [Bar]	Time [hr]	PO	BO	CHO	SO	ECH	GLY	Reference
OMe-OH-TPBP-COF	40	1	24	90	86	-	-	91	-	<a href="#">4</a>
Cu <sub>x</sub> O <sub>y</sub> @COF	40	1	12	92	-	95	91	98	94	<a href="#">5</a>
MOF-5	50	60	4	95	-	-	92	93	-	<a href="#">6</a>
UiO-66-BAT <sup>b</sup>	50	5	12	95	92	-	93	-	-	<a href="#">7</a>
Ru-HKUST-1	50	7	24	93	73	52	94	97	57	This Work
NUC-51a	55	1	6	99	98	-	97	-	-	<a href="#">8</a>
TbL	70	10	12	46	-	37	89	>99	-	<a href="#">9</a>
NUC-53	80	1	4	99	99	-	99	99	-	<a href="#">10</a>
Nu-1000(Zr)	80	4	4	98	97	4	98	95	-	<a href="#">16</a>
MOF-801(D)	80	1	15	91	-	18	87	92	-	<a href="#">17</a>
NH <sub>2</sub> -MIL-101(Al)	120	18	6	96	98	15	>99	-	-	<a href="#">13</a>
UMCM-1-NH <sub>2</sub>	120	12	24	90	-	10	53	78	-	<a href="#">14</a>

<sup>a</sup> = TBAB as co-cat    <sup>b</sup> = TBAI as co-cat    - = not reported

## SI 5. References

1. W.-Y. Gao, Y. Chen, Y. Niu, K. Williams, L. Cash, P. J. Perez, L. Wojtas, J. Cai, Y.-S. Chen and S. Ma, *Angewandte Chemie International Edition*, 2014, **53**, 2615-2619.
2. S. G. Musa, Z. M. Aljunid Merican and O. Akbarzadeh, *Polymers (Basel)*, 2021, **13**.
3. K. Kiatkittipong, M. A. A. Mohamad Shukri, W. Kiatkittipong, J. W. Lim, P. L. Show, M. K. Lam and S. Assabumrungrat, *Processes*, 2020, **8**, 548.
4. F. Yang, Y. Li, T. Zhang, Z. Zhao, G. Xing and L. Chen, *Chemistry – A European Journal*, 2020, **26**, 4510-4514.
5. M. Sengupta, A. Bag, S. Ghosh, P. Mondal, A. Bordoloi and S. M. Islam, *Journal of CO2 Utilization*, 2019, **34**, 533-542.
6. J. Song, Z. Zhang, S. Hu, T. Wu, T. Jiang and B. Han, *Green Chemistry*, 2009, **11**, 1031-1036.
7. A. Helal, M. Usman, M. E. Arafat and M. M. Abdelnaby, *Journal of Industrial and Engineering Chemistry*, 2020, **89**, 104-110.
8. H. Lv, L. Fan, H. Chen, X. Zhang and Y. Gao, *Dalton Transactions*, 2022, **51**, 3546-3556.
9. T. Jing, L. Chen, F. Jiang, Y. Yang, K. Zhou, M. Yu, Z. Cao, S. Li and M. Hong, *Crystal Growth & Design*, 2018, **18**, 2956-2963.
10. H. Chen, S. Liu, H. Lv, Q.-P. Qin and X. Zhang, *ACS Applied Materials & Interfaces*, 2022, **14**, 18589-18599.
11. M. N. Timofeeva, I. A. Lukoyanov, V. N. Panchenko, K. I. Shefer, M. S. Mel'gunov, B. N. Bhadra and S. H. Jung, *Molecular Catalysis*, 2022, **529**, 112530.
12. D. H. Le, R. P. Loughan, A. Gładysiak, N. Rampal, I. A. Brooks, A.-H. A. Park, D. Fairen-Jimenez and K. C. Stylianou, *Journal of Materials Chemistry A*, 2022, **10**, 1442-1450.
13. S. Senthilkumar, M. S. Maru, R. S. Somani, H. C. Bajaj and S. Neogi, *Dalton Transactions*, 2018, **47**, 418-428.
14. R. Babu, A. C. Kathalikkattil, R. Roshan, J. Tharun, D.-W. Kim and D.-W. Park, *Green Chemistry*, 2016, **18**, 232-242.
15. V. Abdelsayed, T. H. Gardner, A. H. Kababji and Y. Fan, *Applied Catalysis A: General*, 2019, **586**, 117225.
16. M. Pander, M. Janeta and W. Bury, *ACS Applied Materials & Interfaces*, 2021, **13**, 8344-8352.
17. Y. Gu, B. A. Anjali, S. Yoon, Y. Choe, Y. G. Chung and D.-W. Park, *Journal of Materials Chemistry A*, 2022, **10**, 10051-10061.